5-2021

Post cleanup composition and geochemical analysis of historic gold processing residues

Owen Daniell
Bates College, odaniell@bates.edu

Follow this and additional works at: https://scarab.bates.edu/geology_theses

Post cleanup composition and geochemical analysis of historic gold processing residues

A Senior Thesis

Presented to

The Faculty of the Department of Geology

Bates College

In partial fulfillment of the requirements for the

Degree of Bachelor of Science

By

Owen B. Daniell

Lewiston, Maine

May 23, 2021

Acknowledgements

Table of Contents

Table of Tables

Table of Figures

Abstract

Before mining ceased, ore-processing residues were piled outside the Callery battery, a gold processing plant in East Otago, New Zealand. These residues were rich in arsenic and mercury. After mining ceased, the site was turned into a historic reserve. In 2005, Mains and Craw investigated the geochemistry of the residues. Unacceptably high concentrations of arsenic were found, prompting the Department of Conservation to clean up the site. This cleanup was successful in decreasing Hg concentrations, but only partially successful with As concentrations. Fe concentrations have drastically increased since 2005. Up to 87000 ppm of As was found, prompting the conclusion that the cleanup was only partially successful.

1 Introduction

1.1 General Geography of New Zealand

New Zealand is in the Southwest corner of the Pacific Ocean, next to Australia. The country consists of

two major islands, the North Island, and the South Island. The South Island is characterized by the

Southern Alps mountain range rising up from the West coast, flat river gravel plains in the Canterbury

region, and hilly basin and range in the Otago region. The Golden Point site is in the Northern part of

Otago. It sits on a hilly area between the Shag river catchment and the Taieri river catchment. To the

North is the flat Canterbury Plain, while to the South and East is the hilly upland of central Otago.

Figure 1.1 General geography of New Zealand. Canterbury plains and Southern Alps are labelled. The study site is marked with a red X (thanks to freeworldmaps.net for this map, URL in references).
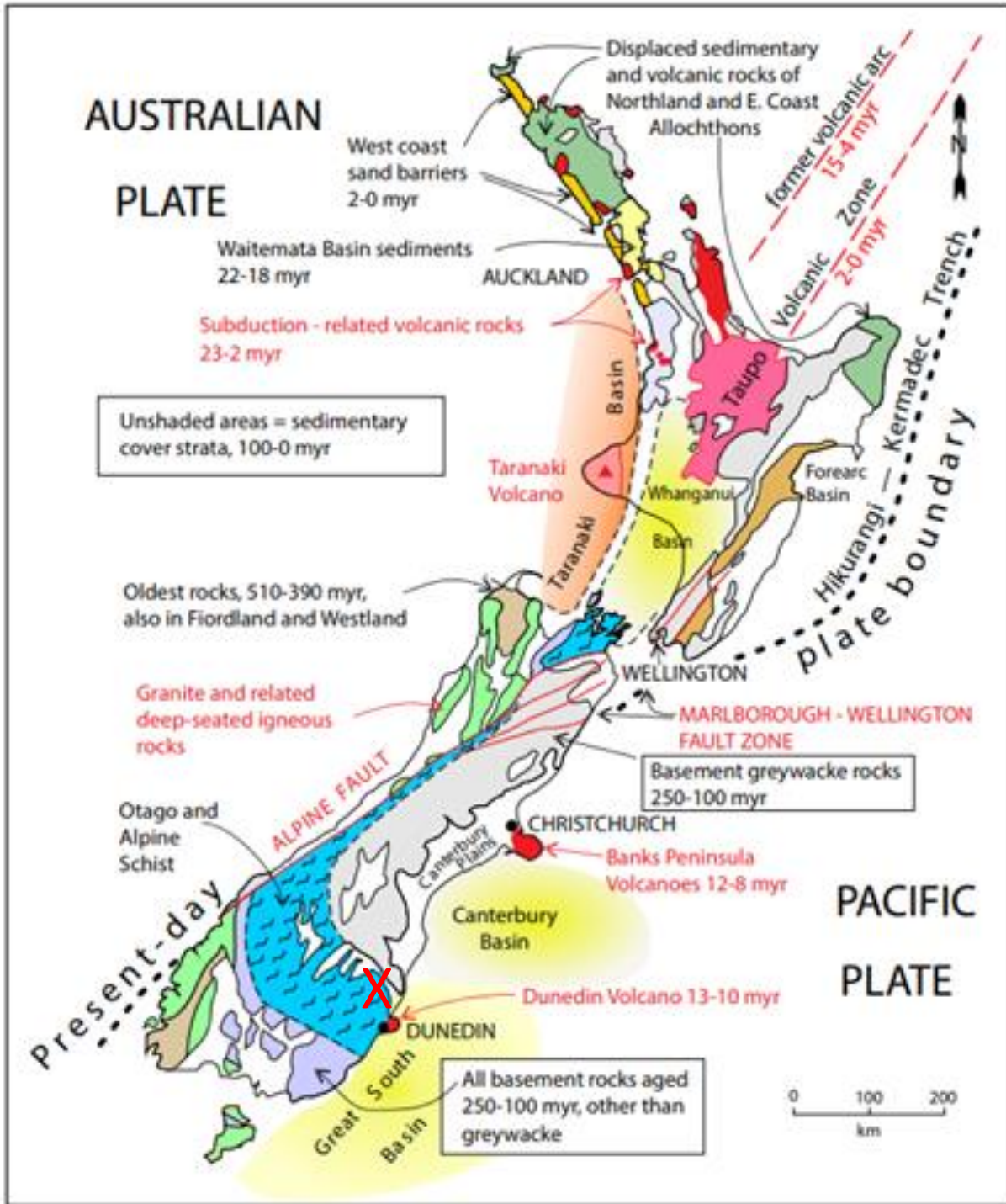
Figure 1.2 New Zealand geology. The site is marked with a red X. GNS science (see references for URL)

1.2 General Geology of New Zealand

New Zealand is a product of the dextral motion of the Pacific plate relative to the Australian Plate. This motion causes a 600km strike slip fault (the Alpine fault) on the west coast of the South Island, and a subduction zone volcanic arc on the North island. The Alpine fault slip and resulting uplift of the Southern Alps has resulted in many amalgamated terranes on the fault's Eastern side (see Figure 1.2)(Craw, Windle et al. 1999). One of these terranes is known as the Otago schist, stretching from Southland to the Northern part of the South Island. The rock unit consists of amalgamated Mesozoic terranes with widely varying metamorphic grades. At the lowest grade, it is weakly cleaved prehinite-pumpellyte, greywackes and argillites. At its most metamorphosed, the rock consists of upper greenschist facies that are multiply deformed and thoroughly crystalized (Craw, Windle et al. 1999).

1.3 Regional Geography

The site of this study is on the South Island near the town of Palmerston (see Figure 1.3). The Golden Point site is drained by Deepdell creek, which in turn flows into the Shag river. The Shag river flows into the Pacific Ocean near Palmerston. Deepdell creek cuts a narrow canyon in the hilly upland until it reaches the flats of the Shag river valley. The area's climate is cool (annual mean temperature 12 degrees C) and semiarid, with precipitation of 500-700 mm per year (Craw and Pacheco 2002). The region is often subject to low humidity winds, and potential evaporation is >700 mm per year. Vegetation tends to be grasses or small shrubs (Craw and Pacheco 2002).
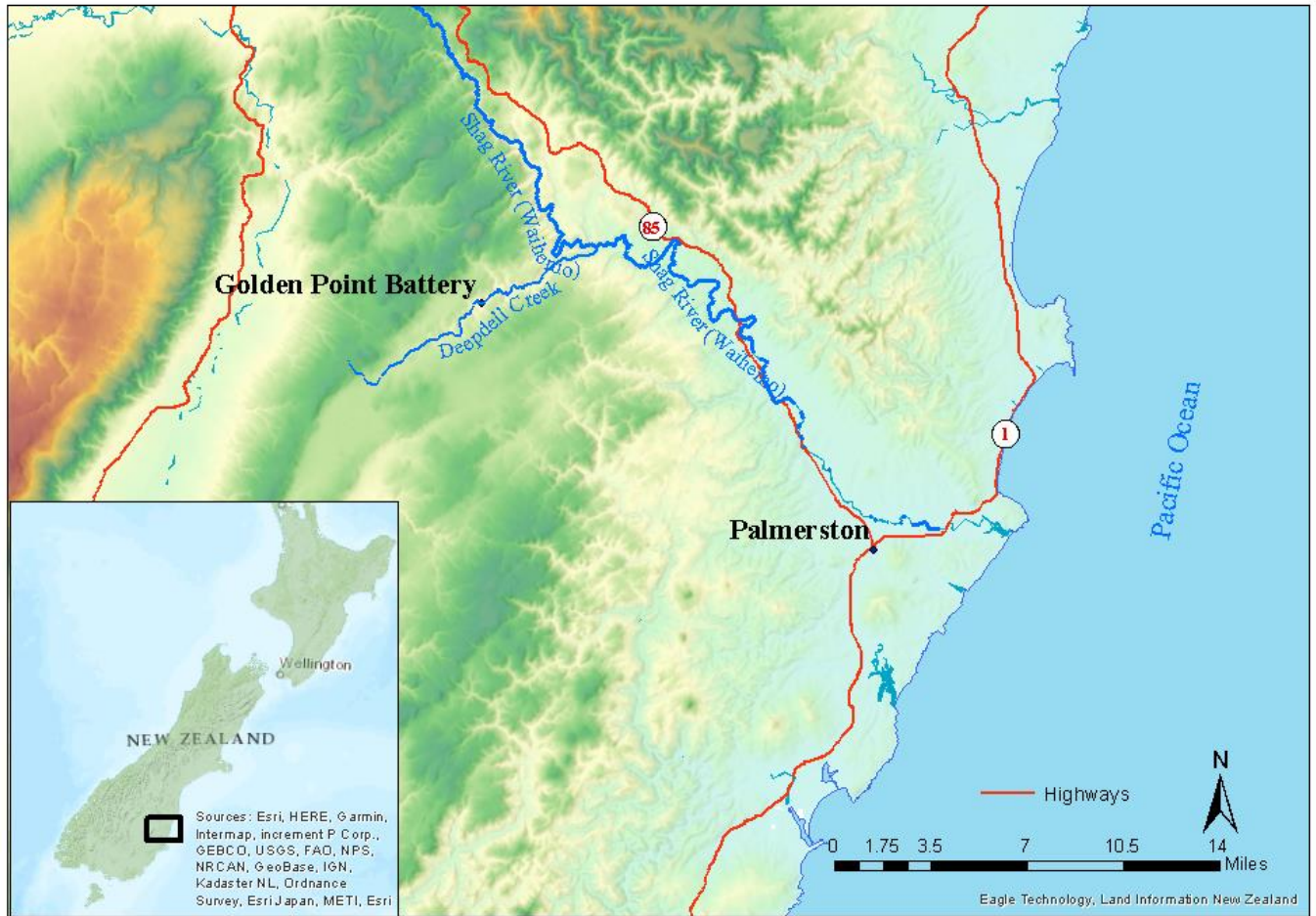
Figure 1.3 map showing Palmerston, the Golden point battery, as well as the waterways draining from the Golden point site.

1.4 Geology of Region

The source of the gold mineralization at the site is the Hyde-Macraes shear zone. The shear zone is around 30 km long, and roughly 10 meters wide at either end. In the center it is up to 120 meters wide. The extent of the shear zone and location of the site within can be seen in Figure 1.4. The shear zone results from thrust faulting between 130 and 140 million years ago. At that time, the zone was around 10-15 km deep (Teagle 1987). The reverse faulting is shown in Figure 1.5.

The rock of the shear zone underwent one phase of gold mineralization involving partially ductile deformation, and then a second phase in which gold bearing quartz veins mineralized (Craw, Windle et al. 1999). The way in which quartz veins mineralized has multiple explanations. There is agreement that hydrothermal liquid containing quartz, gold and sulfides was responsible for the mineralization, but the source of the hydrothermal liquid is attributed to both metamorphic processes and post metamorphic magmatism (Craw, Windle et al. 1999). Gold is contained in both coarse fragments >100 μm in size, and fine fragments (<10 μm). The fine fragments are within sulfide minerals, primarily pyrite ($FeS2$) and arsenopyrite (FeAsS) (Kerr and Craw 2021).
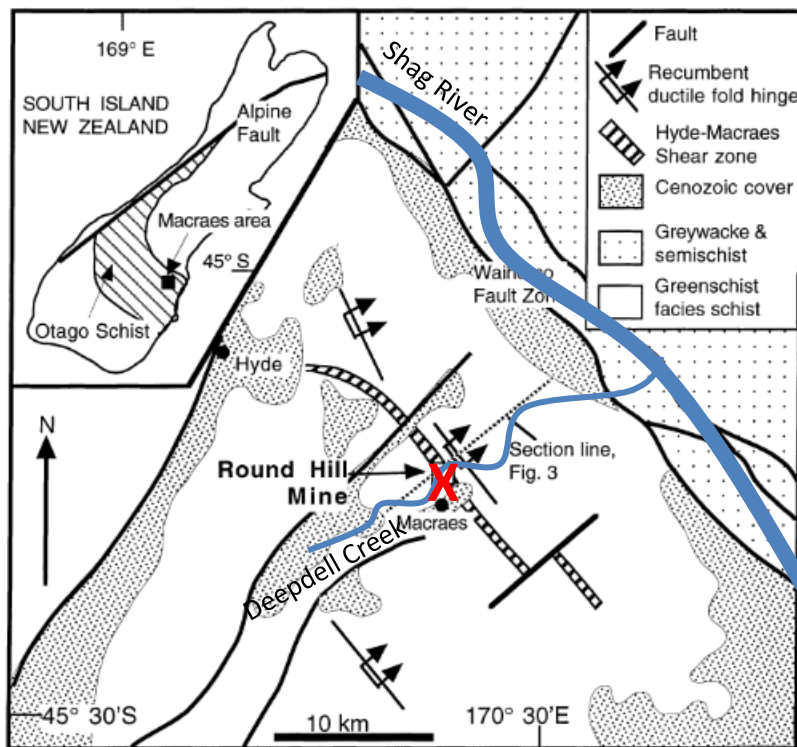
Figure 1.4 The Hyde-Macraes shear zone and surrounding geology (Craw, Windle et al. 1999). The red X shows the Golden Point study site.
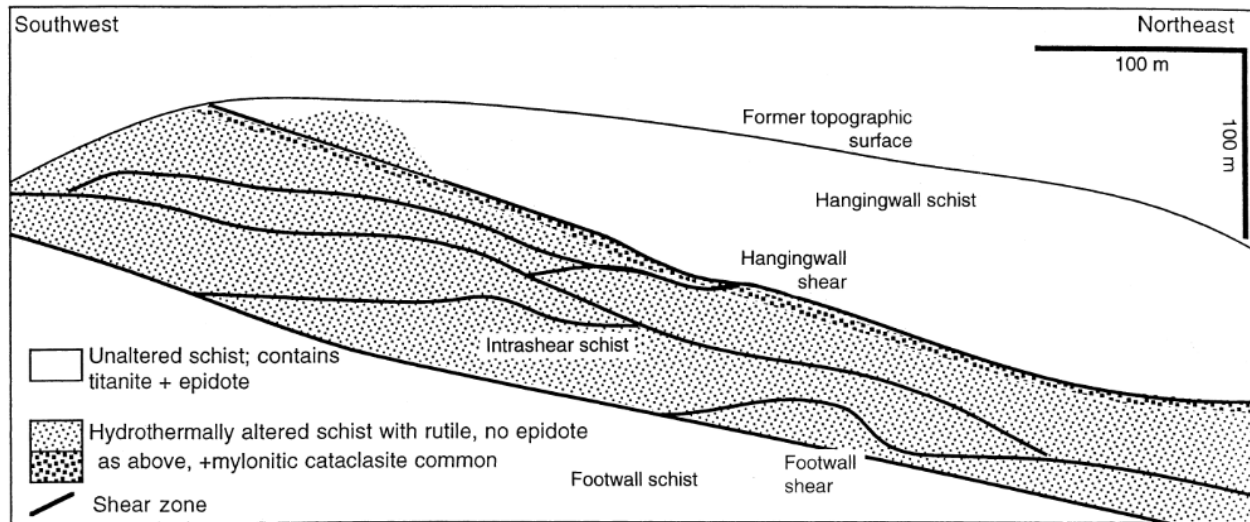
Figure 1.5 a section line of the Hyde-Macraes shear zone. This section is shown in Figure 1.3 as "Section line Fig. 3"(Craw, Windle et al. 1999).

1.5 History of Gold mining

Gold was initially discovered in New Zealand in the early 1800s. Initially, alluvial river gravel deposits were panned by individual miners (Walrond 2006). These easily mined alluvial deposits were soon exhausted, and hard rock mining began. Hard rock mining was significantly more difficult than alluvial mining, and thus miners formed companies instead of working alone (Walrond 2006). This new type of mining also required significant processing of the ore. The buildings erected to do this were known as batteries.

Hard rock mining operations focused on Quartz veins which had the highest gold concentrations. Once a suitable quartz vein had been discovered, an adit, or tunnel, would be dug through the vein, extracting all the ore found within. The rock was then brought from the adit to the processing plant, known as a battery, via cableway to undergo stamping. In stamping, a heavy weight was repeatedly dropped on the ore to crush it into small pieces (Vallance 2019). At the Callery battery there are 4 stamping rods, each weighing a half ton. Each time a rod was raised and dropped, it would force crushed

14

dust through a wire mesh. The dust was then separated by density on a Wilfley table. The dust of a unsuitable density was discarded into the creek (Black, Craw et al. 2004, Vallance 2019). Most operations focused on coarse gold fragments, but later a roasting process was used to extract finer gold from arsenopyrite and pyrite.

Arsenopyrite and pyrite ore were roasted for hours in a coal furnace to oxidize (Mains and Craw 2005, Kerr and Craw 2021). Oxidized sulfide minerals and dust potentially containing gold were then put through a process called mercury amalgamation (Mains and Craw 2005). First, the gold bearing ore was mixed with liquid mercury. This would cause the gold dust to dissolve into the mercury, forming an amalgam. The ore was then discarded, and the amalgam was heated slowly up to 1500 degrees C, until all mercury had boiled away and only gold remained. The Hg was recycled for further use (Velásquez-López, Veiga et al. 2010).

2 Overview

2.1 Environmental Impacts of Gold Mining

There are two primary contaminants studied in this paper: arsenic (As) and mercury (Hg). The two contaminants have different sources in mine tailings. Gold bearing arsenopyrite is the As source rock (Craw, Windle et al. 1999), while Hg is used in the refining process as described above.

The surplus ore is a key contributor to the As of mine tailings (Mains and Craw 2005). In gold processing, large amounts of arsenopyrite ore separated on the Wilfley table are discarded. The weathering of this ore can then cause As to end up in the wider environment.

The Hg amalgam is a key contributor to Hg in the environment. The process of Hg amalgamation recycles the Hg, using a condenser to recover the Hg which boils off (Velásquez-López, Veiga et al. 2010). However, no system is perfect, and there were likely many opportunities for spillage of Hg to occur. Potentially some Hg amalgam could be imperfectly separated from the rest of the ore, resulting in some residual Hg amalgam on the discarded ore. Another possibility is that when the Hg was boiled off and condensed, some escaped the boiler/condenser system and ended up on the ground. Given the equipment of the time, this would not be excessively improbable. (Kerr and Craw 2021).

2.2 As Environmental Geochem

As is common in soils near quartz veins containing arsenopyrite. Soil concentrations are up to 200 ppm(Craw and Pacheco 2002). As(III) and As (V) are the primary naturally occurring As ions (Cullen and Reimer 1989), and their proportions are dependent on the soil pH, the redox potential, and the biological activity (Cullen and Reimer 1989). As (III) is known to be the most toxic species of As (Cullen and Reimer 1989). At low soil pH, the most common Arsenate-bound mineral found in the weathering environment is scorodite (Drahota, Rohovec et al. 2009, Bowell and Craw 2014), which exhibits itself as a tarnish on the outside of Arsenopyrite when the latter is exposed to oxidation (Craw and Pacheco 2002). The scorodite is often supplanted in this tarnish by Fe Oxyhydroxides (Drahota, Rohovec et al. 2009). At

higher pH, goethite is more common than scorodite. Scorodite is insoluble at low pH, but as pH rises, it becomes soluble in water (Mains and Craw 2005). These changing mineral stabilities based on pH are shown in figure 2.1.
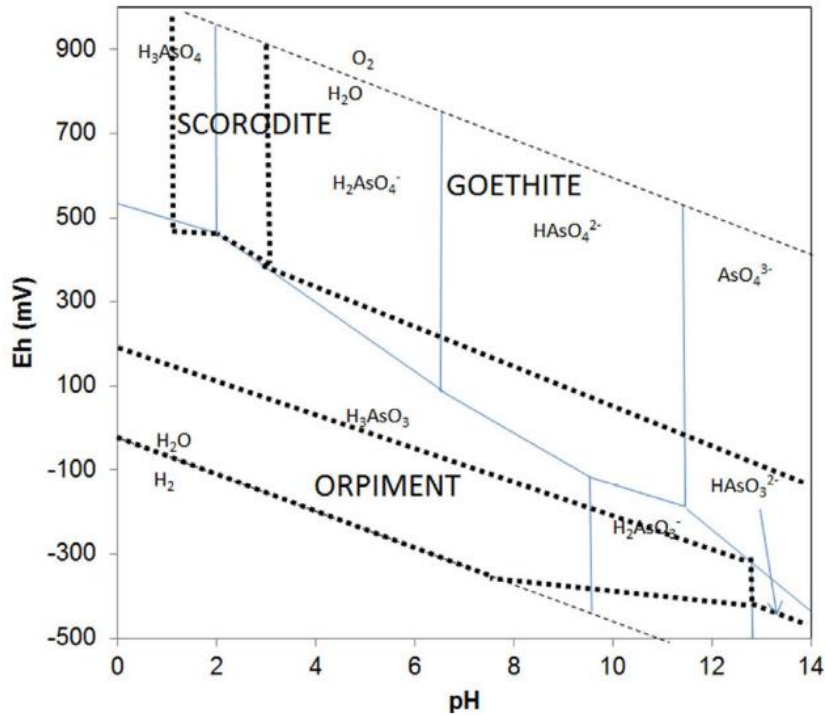
Figure 2.1 The stability of As containing minerals at different Eh (higher Eh means closer to the Earth's surface) and pH (Bowell and Craw 2014).

2.3 Golden Point Battery History

The first battery at the Golden point site was constructed in 1889. A series of several batteries were built in the area in the early 1900s. Processing of the low grade ores was difficult by the techniques of the time (Teagle 1987). By 1960, all but one battery had been turned into scrap. This study focuses on the one remaining battery, known as the Callery battery. After its closing, the battery and surrounding area were turned into a historic reserve by the New Zealand Department of Conservation (DOC). The Callery battery, where this study focuses, is shown in Figure 2.2.

In 1990 the OceanaGold corporation opened a modern mining operation along the Hyde-Macraes shear zone. The modern operation is capable of processing lower grade ore than the battery was (Kerr and Craw 2021) and continues to run both open pit and underground operations. The shear zone has a reserve of around 60 million tons of ore, with 1.58g of gold per ton of ore (Craw, Windle et al. 1999).

Over the 60 years of mining operations at the Golden Point site, more than 85000 tons of mine tailings were dumped into the creek. These were washed down to the Shag river to the Pacific ocean (Black, Craw et al. 2004). Sediment studies from Deepdell creek and the Shag river show elevated As concentrations in sediments, but not excessively so. The highest sediment As concentration found in Deepdell Creek was 250 ppm, and in the Shag river As concentrations were below 25 ppm. As concentrations in the waters of Deepdell creek did not exceed 4 mg/l. These figures indicate that the watercourses which received the tailings are no longer extremely contaminated (Black, Craw et al. 2004).

Despite the relatively small amounts of contamination of nearby watercourses, the tailings which remain on the banks are still sites of significant contamination. In 2005, Mains and Craw examined the tailings residues next to the battery and found very high As concentrations, up to 98000 ppm, or 9.8% As. Hg concentrations as high as 1230 ppm were also found. Concentrations of both elements were particularly high in cemented residues. These findings are detailed in Figures 2.3 and 2.4. In both these figures, one can clearly see more concentrated cemented residues on the top right (orange circle), and the more spread out, less concentrated friable residues to the bottom left (blue circle). The findings of Mains and Craw prompted DOC to undertake a cleanup of the cemented residues (Kerr and Craw 2021). The cleanup removed all the cemented residues, and some of the friable residues. The extent to which this cleanup succeeded in removing the hazardous waste from the Golden Point site is the focus of this study.

Figure 2.2 The Callery Battery, study site, and surrounding area. Deepdell creek flows from the left to right.
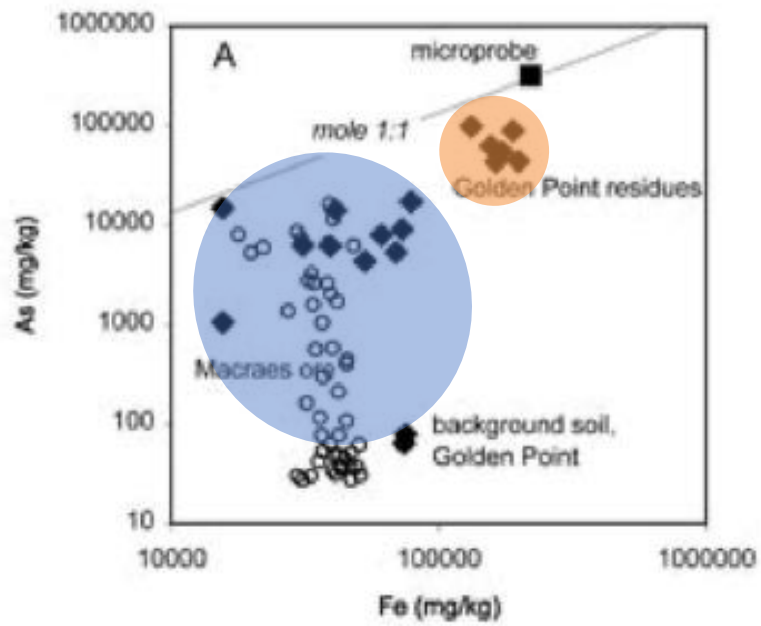
Figure 2.3 The biplot of As and Fe from Mains and Craw 2005
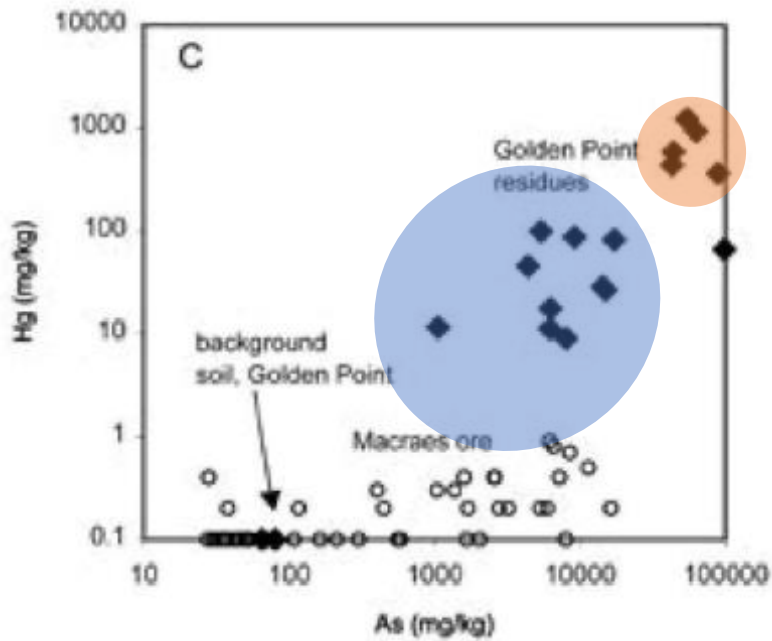
Figure 2.4 The Hg to As biplot from Mains and Craw 2005

20

3 Objectives

The objective of this study is to determine the effectiveness of the 2005 DOC cleanup on As, Fe, and Hg concentrations. This is accomplished by comparing the results of this study with those of Mains and Craw 2005. The differences in these data will help determine whether DOC was successful in making this site safe for recreational use as a historic reserve.

There are several significant elements to this study. As is a widespread poison which is harmful to anyone who ingests it (Bowell, Alpers et al. 2014). Hg is also very biologically toxic (Hazen 2012). The first study into this site (Mains and Craw 2005) prompted a government cleanup due to the extreme contamination uncovered, so this site clearly has significance to its managers. Understanding the effectiveness of the site cleanup will allow for a better understanding of what additional work might be needed to make the site safe and how site cleanup might be accomplished in the future.

4 Methods

4.1 Establishing the Sampling Grid

Element concentration measurements at the site were taken along a series of 11 transects spaced 0.5 m apart. Along the transects, a measurement was taken every 0.5 m. The resultant grid of measurements was 5.5m by 10.5 m. Spatial accuracy was accomplished by laying measuring tapes across the ground, seen in Figure 4.1. Each measurement took around two minutes to complete with the handheld X-ray fluorescence gun, so it would not have made sense to take more than the 230 measurements taken. However, with a 0.5 m interval between measurements, it could be reasonably assured that there would not be too much meaningful data missed by the study. The sample collection was spaced enough to be practicable, but not so widely spaced that key data was missed.

pH data was more difficult to collect, as each measurement took closer to 15 minutes. The way to make this practical was to collect one pH data point for each transect. Some transects had much lower values than others, and the variation in pH with As concentration was a point of interest. Therefore, the pH was collected at the point of highest As concentration in each transect.

Figure 4.1 The Callery battery site during data collection in November 2020. Note measuring tape for one transect on the right side of the photo.

4.2 Elemental Concentrations

A handheld X-ray fluorescence (XRF) spectrometer was used to measure the elemental concentrations of soil. A handheld XRF gun works by shooting X-rays at the sample in question. When an X-ray hits an atom, it excites lower-shell electrons into higher shells. These electrons do not remain excited for long and soon drop back down to their pre-excitement shells. When the electrons do this, they emit X-rays of differing energies. Atoms of each element have a unique arrangement of electrons, and thus a unique signature of X-rays emitted when the electrons return to pre-excitement levels (Sianoudis, Drakaki et al. 2010). The handheld XRF meter uses a detector to measure the energy of incoming X-rays and matches the intensity of each X-ray energy level to the known elemental signature. Comparing the measured X-ray

readings to known graphs, the computer comes up with the percentages of each element in the sample (Sianoudis, Drakaki et al. 2010).

4.3 Soil pH

A pH meter measures the concentration of H^+ ions in a solution. To measure soil pH, one part soil was mixed with 2.5 parts distilled water. A pH meter then tested the solution. The meter compares the electric potential of a known-pH solution with the test solution. Because of the difference in H^+ ions, one solution will be more positively charged than the other. An electric field will always point towards a negative charge, and be more intense the bigger the difference in the charges is. Thus, the pH is measured by the difference in electric potential, the integral of the electric field (Purcell and Morin 2013). This potential difference is displayed as a voltage across the glass membrane (Group 2021), and interpreted by the meter's computer to display a pH value.

4.4 Analysis and Comparison

Once samples were collected, analysis began. With a principle focus on As, a heatmap of As concentrations was created. This was difficult since the line orientation was ~ 48 degrees offset from North. The solution was to create a continuous line in GIS which snaked its way through all the measurement locations. The line was then populated with points every 0.5m. The object ID of each point was then matched to that of the corresponding measurement. This was repeated with Fe and Hg. For further analysis and comparison, biplots similar to those created by Mains and Craw were created. Furthermore, pH was graphed against transect maximum As concentration. The surface of the area in the 2020 study was divided into 6 different surface types, all of which are labelled in Figure 4.2.

To better understand the effects of the cleanup, a direct comparison was made to Mains and Craw 2005. The 2005 paper had a map of residue types and the measurements taken. By looking at the North arrow, the scale bar, and the distance to Deepdell creek, the figure was approximated to be in the center of this studied area. The Mains and Craw map superimposed onto the map of measurements in this study is

24

shown in Figure 4.2. A closer look at the Mains and Craw map is shown in Figure 4.3. From this map and the residues described, as well as the accompanying tables in Mains and Craw, a direct comparison between the same surface areas in these two studies could be made. Measurements taken in the same place were compared with one another to give the best view possible of the changes resulting from the cleanup.
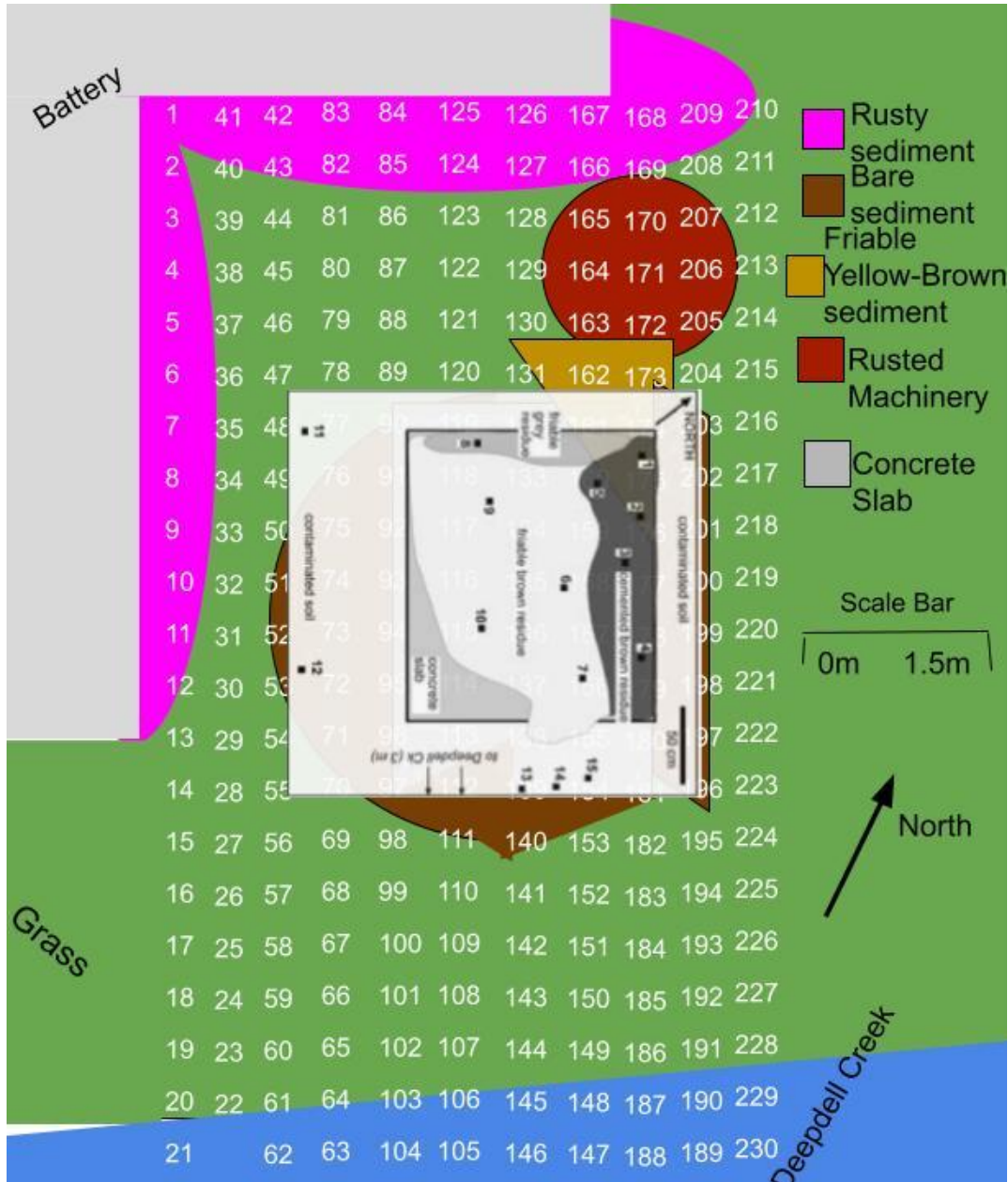
Figure 4.2 the map from Mains and Craw 2005 superimposed on a map of all 2020 measurements and surface types.
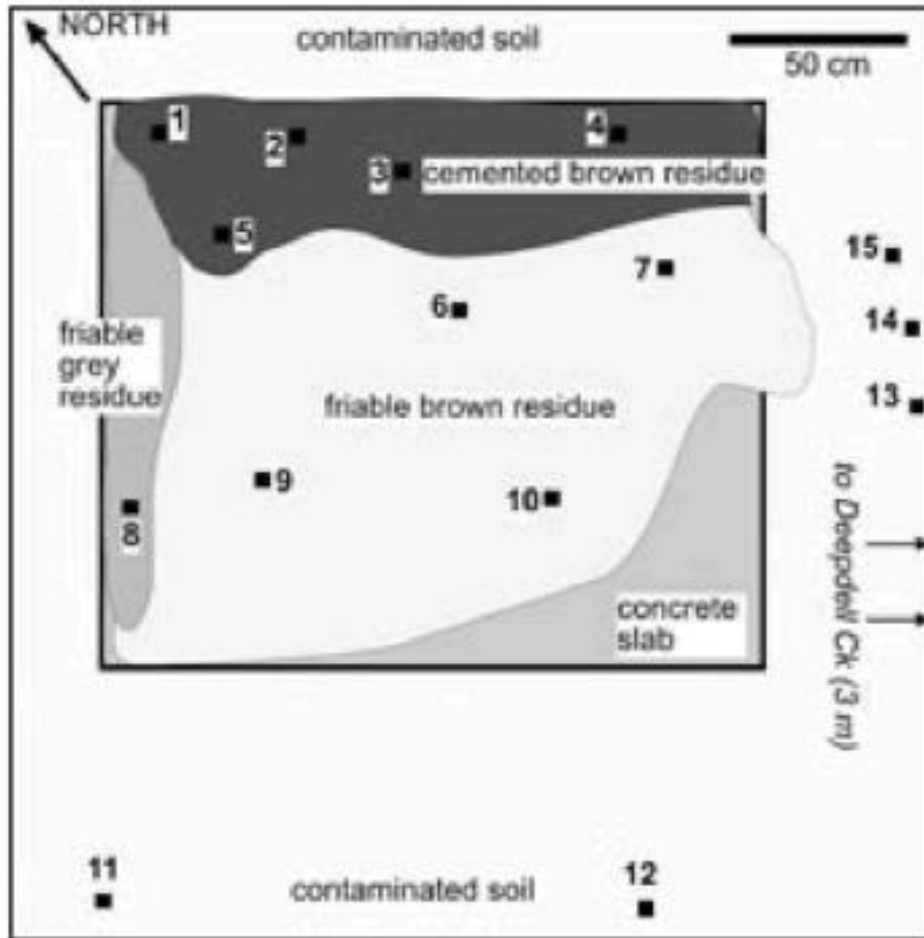
Figure 4.3 The map from Mains and Craw 2005, showing the surface types in the study.

5 Results
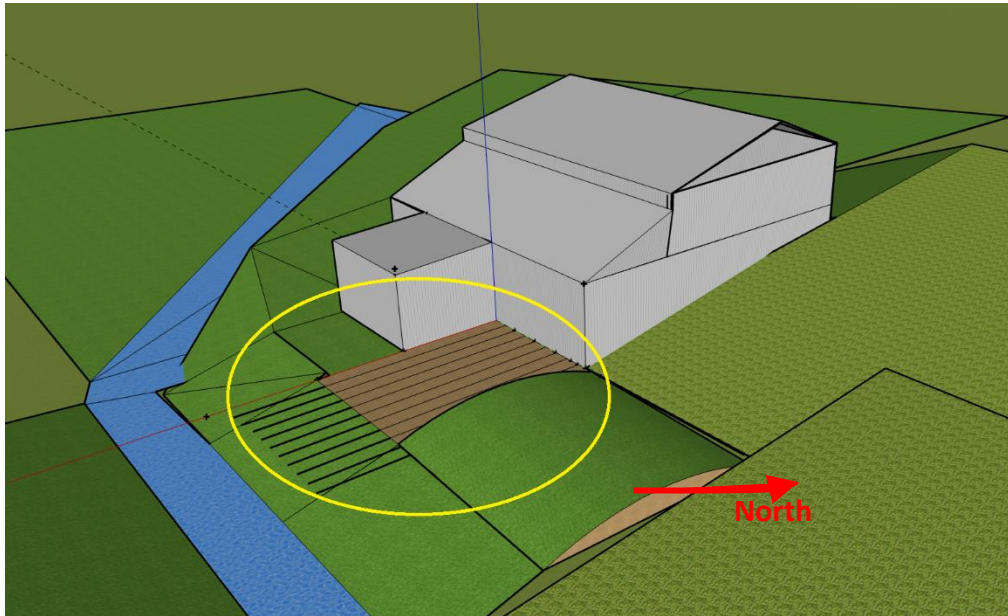
Figure 5.1 the site is shown in a 3D computer rendering, with the transects shown as the black lines within the yellow circle. This gives a better idea of where the site was in relation to the battery and Deepdell creek. Created using Sketchup computer program.

5.1 Surface Type Characterization

The study site can be characterized by six surface types: grass, rusty sediment, bare sediment, concrete slab, friable yellow-brown sediment, and sediment near rusted machinery. The grass had varying distribution, some of it being mowed on a regular basis by DOC as a part of maintenance of the historic reserve, but some of the grass closer to rusted machinery was longer as it could not easily be cut. The rusty sediment was generally next to the battery (refer to Figure 5.2, 5.3) and had a reddish brown tinge. The bare sediment is differentiated from the rusty by being closer to the center of the site and the concrete slab, rather than near the edge of the battery. The most interesting residue for this study is the friable yellow-brown residue on the right hand side of the concrete slab (see Figure 5.2, 5.3). This was a relatively small area, but due to its complete lack of any vegetation, high readings were expected.

27

Figure 5.2 the surface types are labelled on an image from November 2020 during data collection. Rusty sediment is somewhat obscured behind grass and machinery.
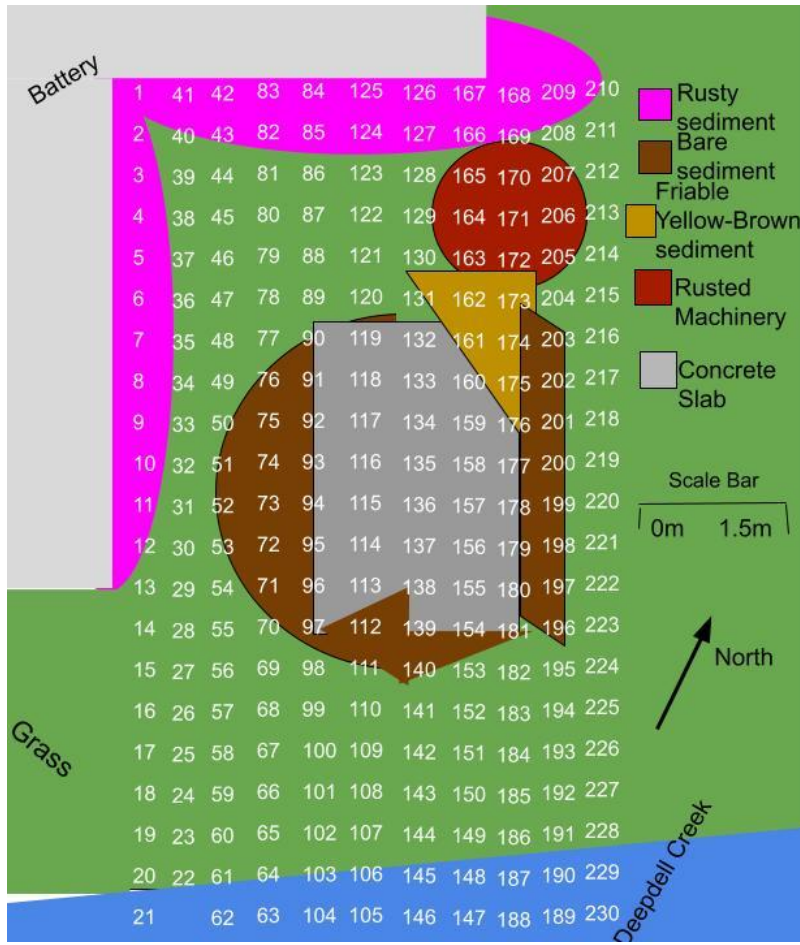
Figure 5.3 A map of the studied area. Each white number represents a site where data was collected.
Some data points look as if they are in Deepdell creek, but those which would have been in the creek
were not collected. However, in order to easily import the points into GIS, it was convenient to assign
object IDs to points that weren't collected.

Type	Surface Type	Fe Concentration (PPM)	As Concentration (PPM)	Hg Concentration (PPM)
AVERAGE 2021	Rusted Machinery	90127.9	16215.4	51.0
	Friable Yellow-Brown Sediment	115675.3	15741.4	84.3
	Concrete Slab	85505.1	14972.9	50.1
	Bare Sediment	30088.5	3990.1	16.2
	Rusty Sediment	46152.8	3930.7	26.4
	Grass	18650.2	1412.2	5.9
AVERAGE 2005	Cemented Residue	175800.0	58440.0	710.8
	Bare Sediment	37540.0	9924.0	18.6
	Friable Yellow-Brown Sediment	81240.0	26842.0	76.6
	Grass	74750.0	72.5	0.1
MAX 2021	Rusted Machinery	424790.0	66379.0	341.0
	Friable Yellow-Brown Sediment	635129.0	87956.0	485.0
	Concrete Slab	333673.0	71133.0	224.0
	Bare Sediment	79956.0	16349.0	55.0
	Rusty Sediment	198230.0	13943.0	90.0
	Grass	126609.0	24241.0	58.0
MAX 2005	Cemented Residue	199000.0	88700.0	1230.0
	Bare Sediment	61100.0	14900.0	28.6
	Friable Yellow-Brown Sediment	132000.0	98300.0	100.0
	Grass	75300.0	80.0	0.1

Table 1 The average and maximum concentrations of each surface type in 2005 and in this study.

5.2 As Concentrations

As concentration was greatest at sites 173 and 159, in the region of the yellow-brown sediment and the concrete slab residue, respectively. The maximum reading was 87000 ppm. Elevated levels were also observed near rusted machinery at concentrations up to 66379 ppm. The rusty edge near the corner of the battery edge also yielded some elevated concentrations at sites 40 and 43, with values ranging up to 13943 ppm. As levels in the grass maxed out at 24241 ppm.
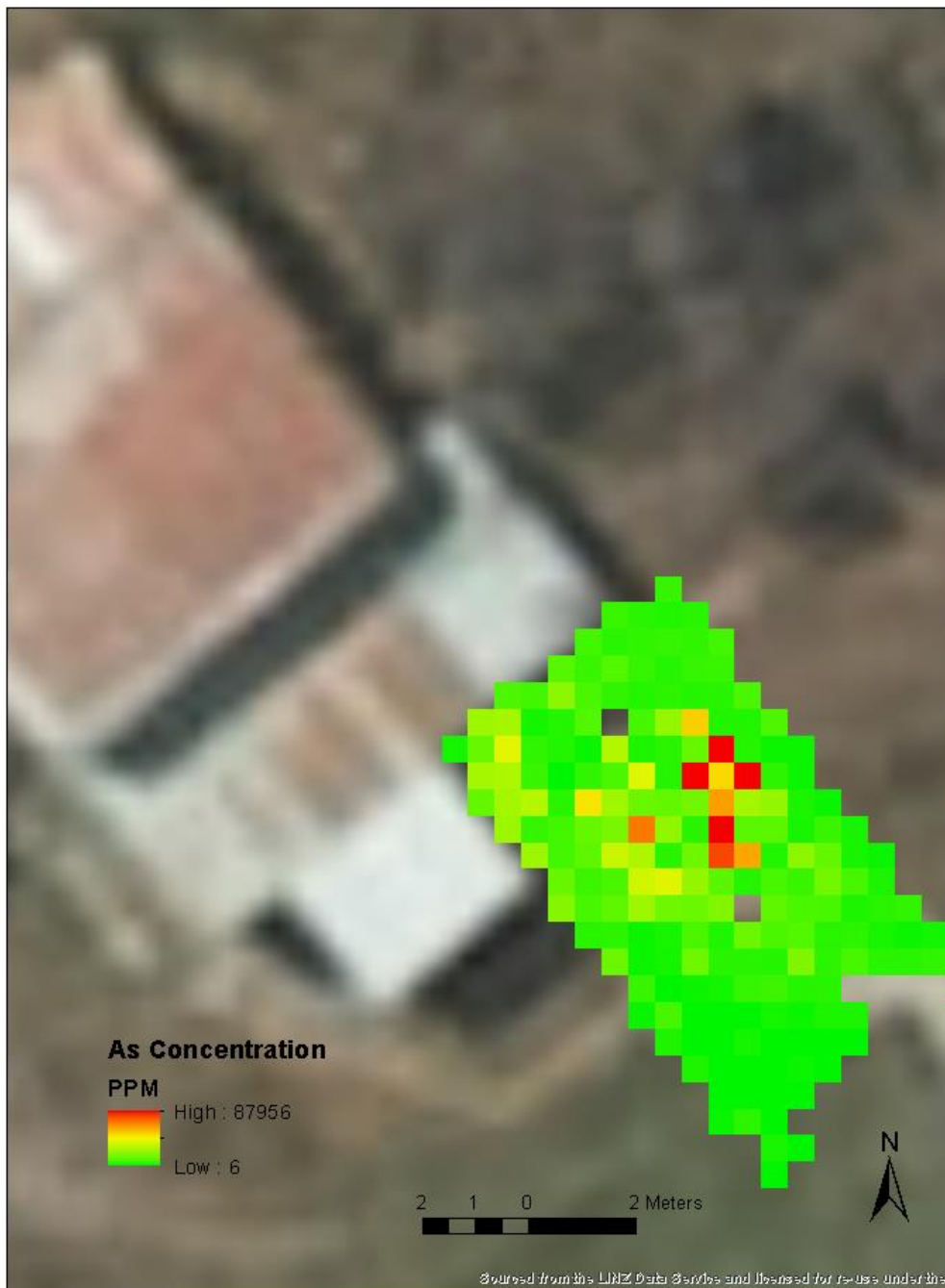
Figure 5.4 A heatmap of As ppm is shown, a section of high concentration can be seen in the cross shape on the right hand side.

Fe Heatmap

Legend

Fe Concentration

PPM

High : 635129

Low : 380
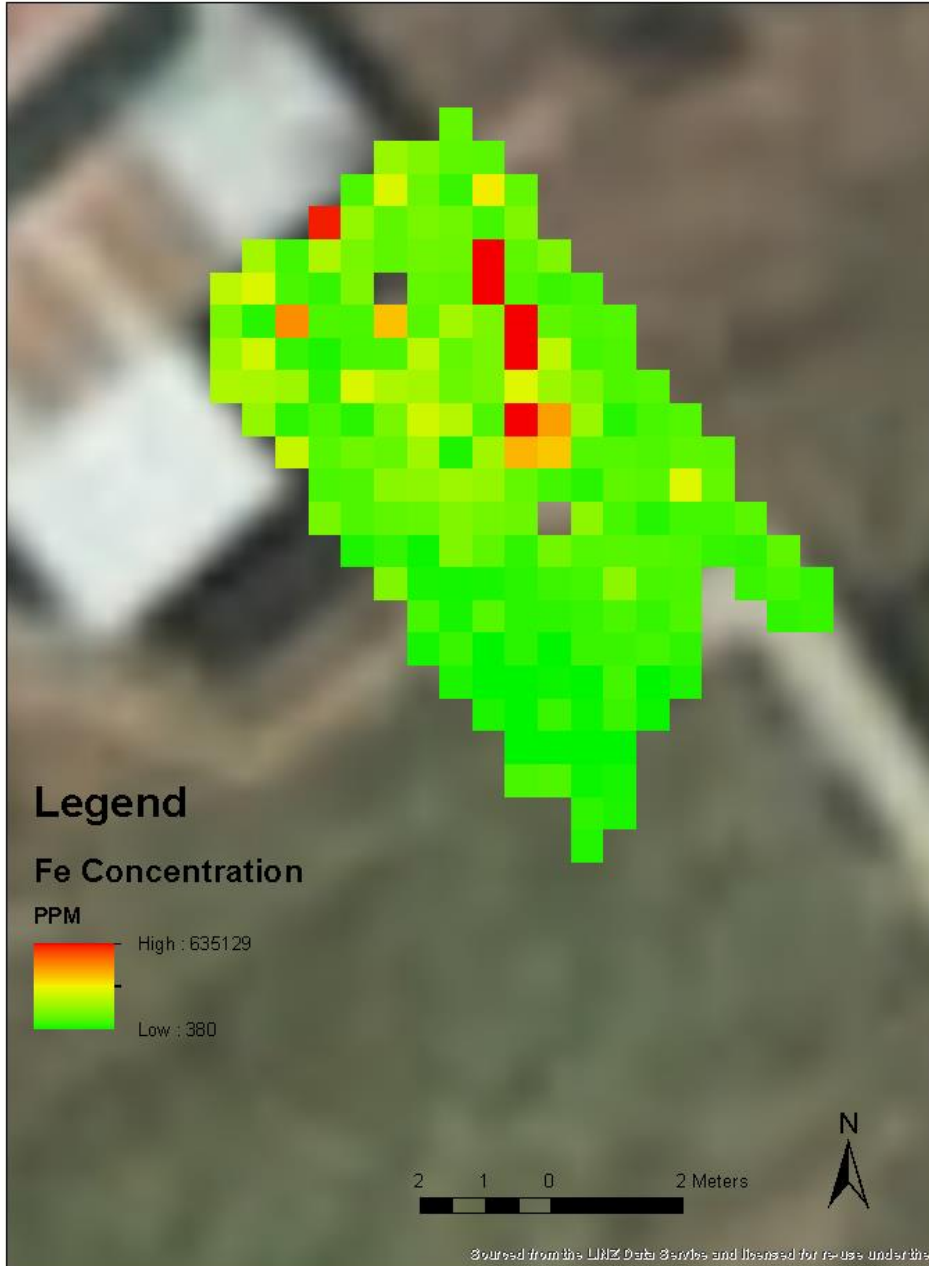
Figure 5.5 The heatmap of Fe is shown, with a section of elevated values shown on the top right.

5.3: Fe Concentration

Fe was the most abundant of the elements studied, with a top concentration of over 635000 ppm, once again at site 173. The upper yellowish sediment has significantly elevated values, with a maximum of 635129 ppm. The residue atop the concrete slab at site 159 with a concentration of 333673. In the rusty sediment area, there is a significantly elevated value of Fe, with a value of 424729 ppm.

Hg Heatmap
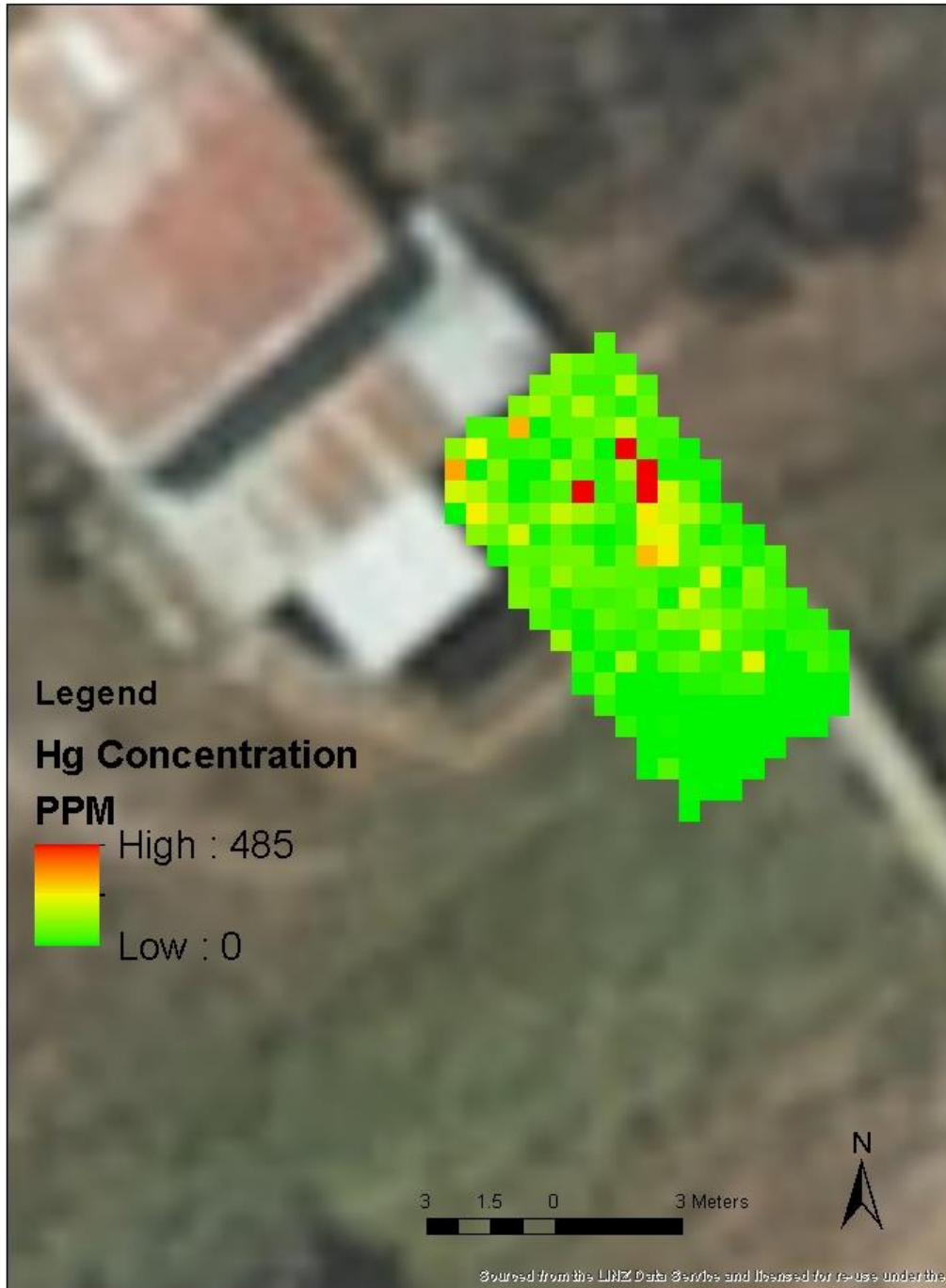
Figure 5.6 Hg concentration is shown, with a clear example of elevated values shown on the top right

5.4: Hg Concentration

Hg concentrations are very low throughout the study area, with a maximum concentration of only 485 ppm. The high was once again at sites 173 and 172. These surfaces were the friable yellow-brown sediment and the rusting machinery. There were also elevated concentrations at site 119 on the concrete slab, as well as a high for the rusty sediment of 90 ppm at site 84.

5.5 As vs Fe
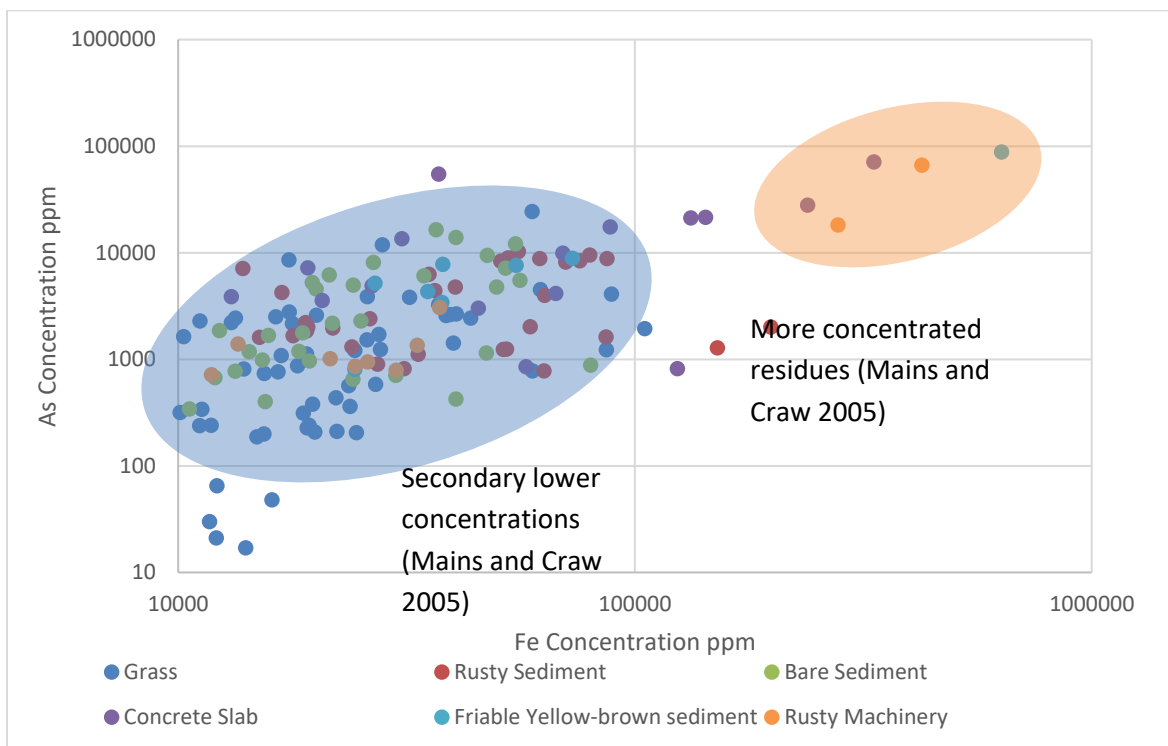
Figure 5.7 A biplot of As and Fe. The secondary lower concentrations and an area of more concentrated residues from Mains and Craw 2005 are labelled on the biplot.

Fe concentrations are mostly below 100000 ppm, just as most As values are below 10000 ppm. However, there are quite a few outliers with As concentrations above 10000 ppm and Fe concentrations above

100000 ppm. Friable yellow-brown sediment has the highest readings for both, followed by rusty machinery and concrete slab.

5.6 Hg vs As
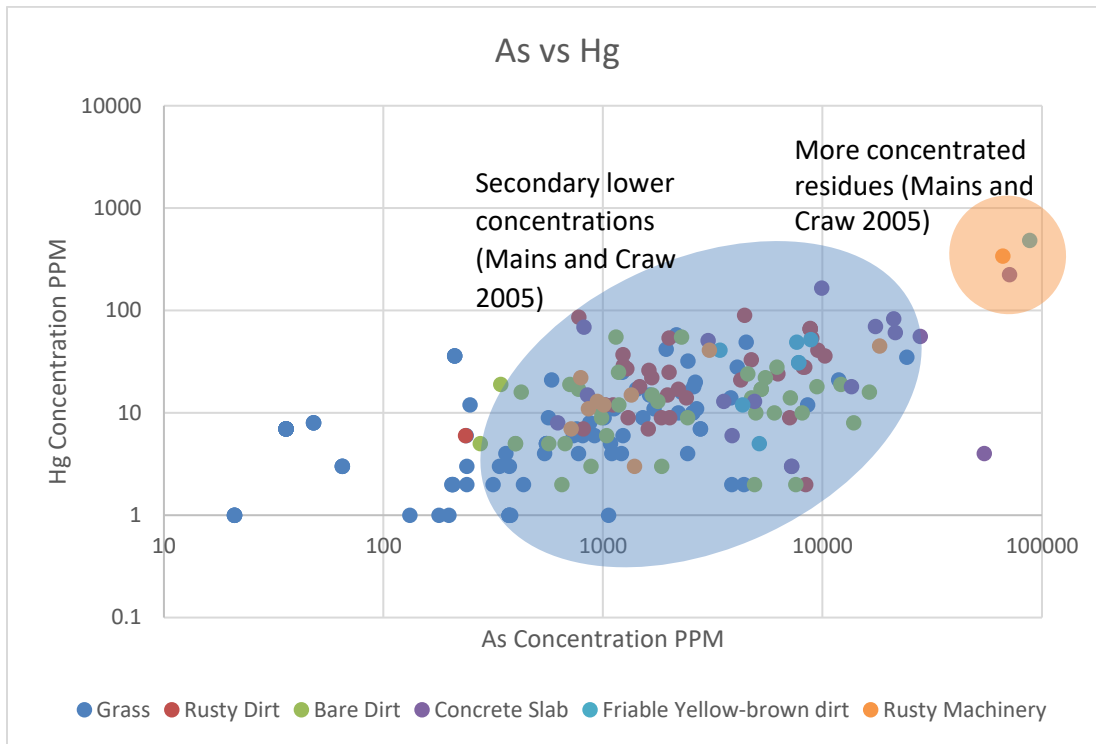
Figure 5.8 the concentration ratios of As and Hg, with the site of each point of elevated reading labelled. The zone each came from is labelled as well. The region where each point falls on the Mains and Craw 2005 graphs is shown in the orange and blue regions.

The ratio between Hg and As is very low, as Hg generally had very low readings. It does, however, show a reasonably strong correlation, and shows elevated values similar to the elevated values seen in the Fe vs As graph. Once again the yellowish sediment and concrete slab residue has the highest readings, while bare sediment to the side of the concrete slab, as well as rusty sediment from near the battery have the next-highest readings.
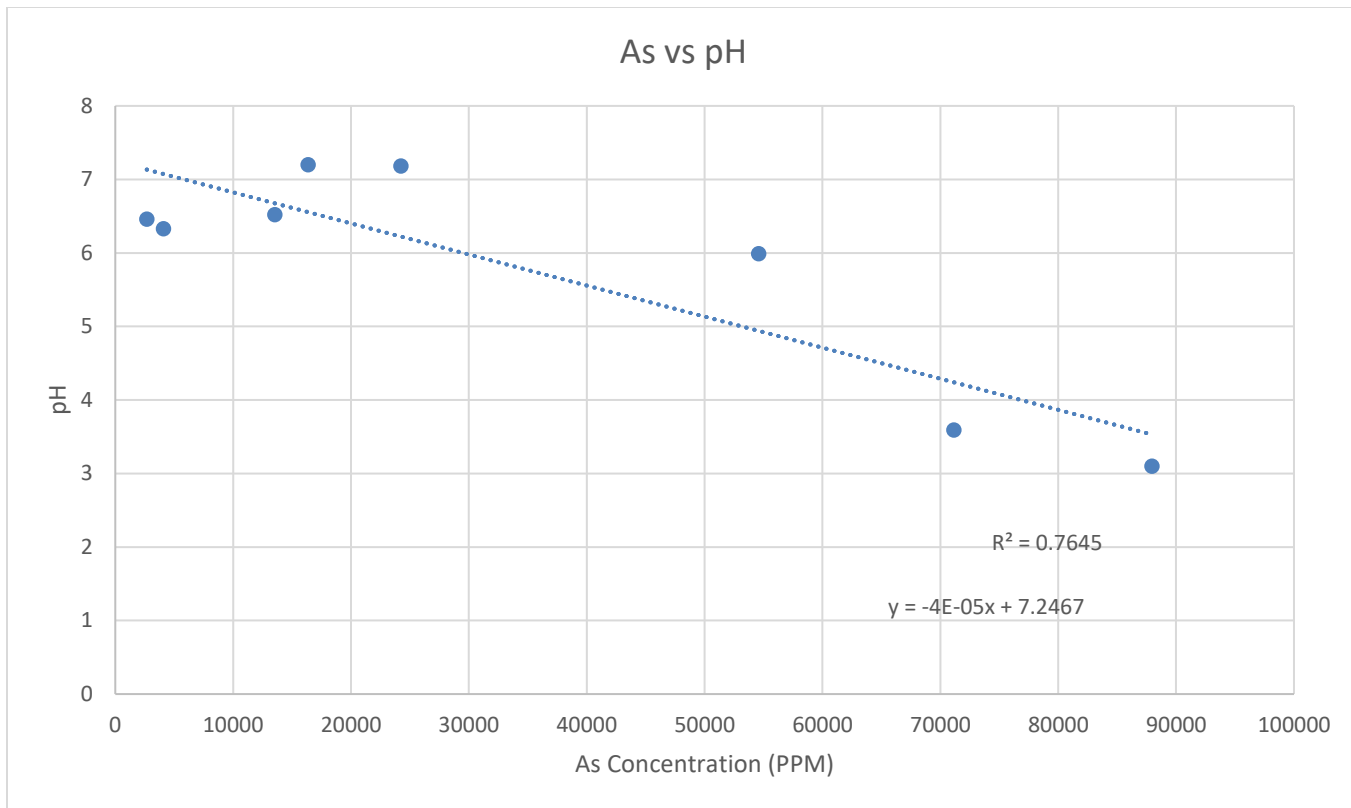
Figure 5.9 As vs pH is shown. Only one pH measurement was taken per line, so the average of each As line is plotted against the line's pH.

6 Discussion

6.1 Discussion Overview

Generally, this study found the 2005 DOC cleanup to be only partially effective. The removal of the cemented residues is evidenced to some degree by reduced contaminant concentrations, but As levels in the surrounding soil are still unacceptably high. Certain areas have much higher contaminant concentrations independent of their soil type, although soil type still likely plays a role in determining concentrations. The toxicity of Hg and As means high concentrations are a real problem for the recreational usability of this site.

6.2 Problematic Concentrations

The ratios seen in this study roughly reproduce those found by Mains and Craw in 2005. The Fe content is consistently higher across the various soil types, but As values tend to be similar (see Table 1). The 2021 data exhibits the same two groups as the data from Mains and Craw 2005. There are a small number of high values to the top right (the orange circle) in both the As vs Fe and As vs Hg graphs (see Figures 2.8, 2.9, 5.7 and 5.8). Circled in blue, there are a larger number of lower As values.

The As to Hg ratio exhibits some change between 2005 and 2021. There are no Hg measurements in 2021 which exceed 1000 ppm, but there are a few around the 1000 ppm mark in the 2005 data. This change is consistent with the idea that the 2005 cleanup removed all the cemented residue from the site. Cemented residue had an average Hg concentration of 710.8 ppm. This is hundreds of ppm higher than the highest value reported in the 2021 data. This leads to the conclusion that the cleanup was successful in decreasing the Hg concentration with the cleanup. The data observed in 2021 is consistent with the secondary "cloud" of values reported by Mains and Craw, but higher concentrations similar to the cemented residue are relatively nonexistent. It can thus be concluded that the cleanup accomplished removal of the cemented residues while secondary residue (the blue circle) remains.

This story continues with the As to Fe ratio. There are only a few measurements that have very high As concentrations, but the Fe concentration seems to have increased since 2005. The Fe concentration in 2005 was a maximum of 199000 ppm, while in 2021 the highest reading was 635129 ppm. The change in averages is a similar story, with an increase from 81240 ppm average in friable yellow-brown sediment to 115675 ppm in 2020 in the same surface type (see table 1). As has little significant change in maximum values (the max recorded by Mains and Craw 2005 was 98300 ppm in friable yellow brown sediment, while the max recorded in 2021 was 87956 ppm in the same surface type), but the average values in 2021 are starkly lower, with an average of only 15741.4 ppm in friable yellow brown sediment. These data suggest that the Fe concentration has somehow increased, but this is of little concern to the cleanup success as Fe is not a toxic element. These data also suggest that there are still areas of concentrated As, but the overall average has dropped significantly. This is once again consistent with the idea that after 2005 most cemented residue was removed from the site, but the secondary, friable residue remained.

For a recreational area, 87000 ppm is a very high As value. The Crown research institute lists 80 ppm as the soil contaminant standard for recreation under the National Environmental Standard for Assessing and Managing Soil Contaminants for the protection of human health (NES) (Environment 2012). The highest As value found at the golden point site is more than 1000 times the permissible value for recreation. The average of the cleanest areas, those with grass, had more than 10 times the 80 ppm accepted value. These are both indications that the government cleanup was not successful in cleaning up the site, and that As contamination remains a problem to this day.

6.3 Contamination vs Surface Type

Though it is clear to see certain areas have higher contaminant concentrations on heatmaps, these high readings are not confined to one surface type. Some have higher averages than others, but high

concentrations are spread out among multiple surface types in the same area. With the knowledge that contamination of As and Hg shares a common origin (the mine tailings), there must have been some process which caused contamination of nearby surfaces

6.4 Changes in Concentration and Distribution

At least some of the imprecise distribution of As can be attributed to chemical weathering. Much of the ore involved is arsenopyrite. When exposed to oxidation, the exterior of arsenopyrite pieces become tarnished with scorodite (Drahota, Rohovec et al. 2009). Every piece of rock in the mining process was crushed, and therefore would have the opportunity for oxidation due to an exponential increase in surface area. Scorodite is insoluble at low pH, but as pH rises, becomes soluble in water (see figure 2.1). The continued dissolution of pyrite in the mine tailings keeps the pH low, and the scorodite stays stable. However, once the pyrite dissolves completely, the pH increases and the scorodite is no longer stable. Once tailings gain a more neutral pH, the scorodite will dissolve in rainwater and As will be released (Mains and Craw 2005). Thus, the tailings must remain acidic to avoid As spreading from the scorodite. The graph of As vs pH in figure 5.9 supports this claim, as lower pH areas tend to have higher levels of As.

A second potential way that As was spread out is by plant life. Plants can fix or take up As into their biomass. Most native plants are only capable of fixing 1-2 ppm of As, but an exotic weed, *Hieracium pilosella*, has As concentrations in its biomass of up to 18 ppm when growing in soil with 150 ppm (Craw and Pacheco 2002). Once the plant dies, its biomass could be transported by wind or water more easily than As bearing rock or sediment. A single plant at the site is unlikely to be responsible for the whole of As redistribution, but multiple generations of *Hieracium pilosella,* growing over the 70 years between the end of mining activity and this study could have a meaningful effect.

The rusting, or oxidation of iron machinery in the vicinity is likely to blame for the increased levels of Fe. Every piece of machinery had some sort of rust on it (see Figure 5.2), and much of the sediment not covered by grass had a distinct rusty tinge. On the East side of the Southern Alps, there is little precipitation in North Otago at the Golden Point site so rusting would not occur as quickly as in a wetter environment (Craw and Pacheco 2002). The decomposition of the scorodite, by the process described in the previous paragraph, could also play a role in increasing the Fe levels in the soil.

Hg redistribution could have occurred via small droplets flowing as a liquid. Given that Hg is liquid at room temperature, it is possible that Hg changes could be partially explained by the Hg flowing from one place to another. In the cementations which were removed, Hg was found in small droplets within microlayers in the cementation (Kerr and Craw 2021). Other Hg is primarily stored in Schuetteite $(Hg_3(SO_4)O_2)$ (Holley, Craw et al. 2010, Kerr and Craw 2021), a thin surface coating which could easily be weathered away and moved (Hazen 2012). The slight decrease in Hg amounts in all soil types studied by Mains and Craw could likely be accounted for by the physical weathering away of schuetteite and the flowing of liquid Hg droplets.

Incomplete cleanup is another key way for redistribution to occur. When soil and cemented residues were removed, it is likely that spillage occurred. This could result in small pieces of high concentration residue being dropped in areas away from their source. Cemented residues would likely have to be broken up to be transported away from the site, and this process (both breaking and transport) present multiple opportunities for residues to be redistributed.

The changes in As, Fe and Hg cannot be fully explained by either natural factors or the cleanup. There is therefore a significant possibility for further work at this site. A more in-depth mineralogical analysis of the residues would help determine what exactly they are, and residues could also be tested to see to what extent weathering affected their concentrations of As, Fe, and Hg. This mineralogical analysis could assign causes to the elemental change with a reasonable degree of certainty.

7 Conclusion

The bare sediment's average As concentration saw a threefold decrease since the 2005 study, likely due to the DOC cleanup efforts. As described above, the Hg concentration also decreased significantly since the cleanup. The Fe increase, however, is unlikely to be attributed to incomplete cleanup. Unless cemented residue was selectively spilled as to only put Fe into the soil, the cleanup would have similar effects on the Fe concentration as it did on the As concentration.

The Hg concentration had a slight decrease in concentration in the bare sediment surface type, from an average of 18 to 16 ppm. The maximum had a marked increase, but this could likely be explained by experiment methods. The Mains and Craw paper took around 20 measurements, while this paper took 230. One is bound to find a higher data point the more data points one takes.

The friable yellow-brown sediment was also ripe for comparison between the Mains and Craw data and the 2021 data. The Fe concentration average increased from 2005 to 2020, from 81240 to 1156875 ppm. This could likely be attributed to rusting machinery during the 16 years between studies. The maximum Fe values are also higher in this study than the 2005 study. As is the case with Hg, this could be attributed to the greater number of measurements in the 2020 study, and the statistical fact that one will find a wider distribution of values when more values are taken. The Fe concentration in the grassy areas is far higher in the 2021 study, likely because the grassy areas studied in 2005 were further from the site, and primarily studied as background soil tests. This comparison is, however, useful for understanding the difference between the recent grass concentrations and that of the background soil.

The As concentration exhibited a marked decrease between the 2005 and 2021 studies. The average friable yellow-brown sediment concentration in 2005 was 26842 ppm, while in 2021 the average was 15741 ppm. An average decrease of roughly 10000 ppm is a significant change over 15 years. Maximum values also exhibited a decrease of around 10000 ppm, from 98300 to 87956 ppm. This is particularly significant as the 2005 study collected far fewer data points than the 2021 study.

Overall, although the DOC cleanup was successful in decreasing As and Hg concentrations, it did not do so to a sufficient extent with As concentrations as to make the site safe for its new purpose. The cleanup removed the cemented residues which had the highest concentrations, but friable residue which has high concentrations still remains. Although Hg is within the limits of 1800 ppm (Environment 2012), the As is far greater than the 80 ppm standard for a recreational area. To make this a safe site, more remediation and cleanup work is clearly needed.

References

Black, A., et al. (2004). "Natural recovery rates of a river system impacted by mine tailing discharge:

Shag River, East Otago, New Zealand." Journal of Geochemical Exploration **84**(1): 21-34.

Bowell, R. J., et al. (2014). "The Environmental Geochemistry of Arsenic — An Overview —." Reviews in Mineralogy and Geochemistry **79**(1): 1-16.

Bowell, R. J. and D. Craw (2014). "The Management of Arsenic in the Mining Industry." Reviews in Mineralogy and Geochemistry **79**(1): 507-532.

Craw, D. and L. Pacheco (2002). "Mobilisation and Bioavailability of Arsenic Around Mesothermal Gold Deposits in a Semiarid Environment, Otago, New Zealand." TheScientificWorldJournal **2**: 308-319.

Craw, D., et al. (1999). "Gold mineralization without quartz veins in a ductile-brittle shear zone, Macraes Mine, Otago Schist, New Zealand." Mineralium Deposita **34**: 382-394.

Cullen, W. R. and K. J. Reimer (1989). "Arsenic speciation in the environment." Chemical Reviews **89**(4): 713-764.

Drahota, P., et al. (2009). "Mineralogical and geochemical controls of arsenic speciation and mobility under different redox conditions in soil, sediment and water at the Mokrsko-West gold deposit, Czech Republic." Science of The Total Environment **407**(10): 3372-3384.

Ministry for the Environment. 2012. Users' Guide: National Environmental Standard for Assessing and Managing Contaminants in Soil to Protect Human Health. Wellington: Ministry for the Environment

Group, H. R. (2021). "How does a pH meter work?" Iowa St Univerity Holme Research group.

Hazen, R. M., Golden, J., Downs, R.T., Hystad, G., Grew, E.S., Azzolini, D., Sverjensky, D.A. (2012). "Mercury (Hg) mineral evolution: A mineralogical record of supercontinent assembly, changing ocean geochemistry, and the emerging terrestrial biosphere." American Mineralogist **97**(7): 1013-1042.

Holley, E. A., et al. (2010). "Natural and mining-related mercury in an orogenic greywacke terrane, South Island, New Zealand." New Zealand Journal of Geology and Geophysics **53**(2-3): 103-114.

Kerr, G. and D. Craw (2021). "Metal redistribution during cementation of historic processing residues, Macraes gold mine, New Zealand." New Zealand Journal of Geology and Geophysics **64**(1): 120-132.

Mains, D. and D. Craw (2005). "Composition and mineralogy of historic gold processing residues, east Otago, New Zealand." New Zealand Journal of Geology and Geophysics **48**(4): 641-647.

Purcell, E. M. and D. J. Morin (2013). "Electricity and Magnetism." **3**.

Sianoudis, I., et al. (2010). "Educational x-ray experiments and XRF measurements with a portable setup adapted for the characterization of cultural heritage objects." <u>European Journal of Physics</u> **31**: 419.

Teagle, D. (1987). "Structural controls on gold mineralisation in the Hyde-Macraes Shear Zone, East Otago." <u>Otago Geology Theses</u>.

Vallance, N. (2019). "Golden Point Battery." <u>TVNZ Meet the Locals</u> **Season 4 Episode 6**.

Velásquez-López, P. C., et al. (2010). "Mercury balance in amalgamation in artisanal and small-scale gold mining: identifying strategies for reducing environmental pollution in Portovelo-Zaruma, Ecuador." <u>Journal of Cleaner Production</u> **18**(3): 226-232.

Walrond, C. (2006). "Gold and Gold Mining, Otago." <u>Te Ara, The encyclopedia of New Zealand</u>.

Images:

Physical map of New Zealand https://www.freeworldmaps.net/oceania/new-zealand/new-zealand-map-big.jpg

Geologic map of New Zealand. https://nzplaces.nz/tags/Geological-feature, based on https://data.gns.cri.nz/geology/